Determination of the optical band-gap energy of cubic and hexagonal boron nitride using luminescence excitation spectroscopy

2008 J. Phys.: Condens. Matter 20 075233

(http://iopscience.iop.org/0953-8984/20/7/075233)

J. Phys.: Condens. Matter **20** (2008) 075233 (7pp) doi:10.1088/0953-8984/20/7/075233

Determination of the optical band-gap energy of cubic and hexagonal boron nitride using luminescence excitation spectroscopy

D A Evans[1], A G McGlynn[1], B M Towlson[2], M Gunn[1], D Jones[1], T E Jenkins[1], R Winter[1] and N R J Poolton[3,4]

[1] Institute of Mathematical and Physical Sciences, Aberystwyth University, Aberystwyth SY23 3BZ, UK
[2] School of Electrical Engineering and Electronics, The University of Manchester, Manchester M60 1QD, UK
[3] Synchrotron Radiation Department, STFC Daresbury Laboratory, Daresbury, Warrington, Cheshire WA4 4AD, UK

E-mail: ngp@aber.ac.uk

Received 13 September 2007, in final form 10 January 2008
Published 31 January 2008
Online at stacks.iop.org/JPhysCM/20/075233

Abstract
Using synchrotron-based luminescence excitation spectroscopy in the energy range 4–20 eV at 8 K, the indirect Γ–X optical band-gap transition in cubic boron nitride is determined as 6.36 ± 0.03 eV, and the quasi-direct band-gap energy of hexagonal boron nitride is determined as 5.96 ± 0.04 eV. The composition and structure of the materials are self-consistently established by optically detected x-ray absorption spectroscopy, and both x-ray diffraction and Raman measurements on the same samples give independent confirmation of their chemical and structural purity: together, the results are therefore considered as providing definitive measurements of the optical band-gap energies of the two materials.

1. Introduction

Boron nitride has several polytypes, the most common being hexagonal and cubic (h-BN, c-BN respectively) whose structures are akin to their carbon equivalents, graphite and diamond. The mechanical properties of the corresponding BN and C materials are similar, but the electronic properties are significantly different. Unlike carbon, where diamond is a wide-gap semiconductor but graphite is semi-metallic, theoretical studies of the BN electronic structures [1–5] reveal that both c-BN and h-BN are indirect wide band-gap semiconductors, although h-BN has a quasi-direct transition at either the H or K symmetry point. This has important implications when considering practical applications based on these semiconductors.

In order to develop BN as a UV optoelectronic material, it is important to reliably determine the magnitude and nature of the optical band-gap energy, E_g. Electronic structure calculations generally tend to underestimate the observed band-gap energies and there is a considerable spread in the experimentally-determined values of E_g for both h-BN and c-BN. For example, optical absorption and reflectance measurements give values for c-BN ranging from 6.1 eV [6] to >6.4 eV [7], and for h-BN, values quoted are from 4.02 eV [8] to between 4.3 and 6.0 eV [9, 10]. Alternative non-optical measurement methods have also been reported: by using soft x-ray emission spectroscopy, a value of 6.2 eV was determined for c-BN [11], and for h-BN, inelastic electron scattering measurements yielded a band-gap energy of 5.9 eV [12].

The spread of quoted values may be due to factors such as varying sample quality or the experimental methods deployed. In this respect, 6 eV is very close to the VUV limit, so the use of standard arc-lamp or tunable laser sources can provide

[4] Author to whom any correspondence should be addressed. Present address: Institute of Mathematical and Physical Sciences, Aberystwyth University, Aberystwyth, Ceredigion SY23 3BZ, UK.

only a partial energy range for probing the band-edge features. Moreover, many standard measurement methods require large smooth surfaces, but high quality single crystals of BN are uncommon, and surface preparation methods are not as well developed as for diamond and graphite (although there has been much recent progress in producing thin films of c-BN for device applications [13, 14]). Nevertheless, based on the large range of quoted values for E_g, it is clear that there is a need for reliable experimental methods for accurately measuring this key parameter on the highest quality bulk materials available. Here we report on the use of synchrotron radiation-stimulated luminescence in order to achieve this. The approach has three main advantages. (i) Luminescence excitation spectroscopy has less stringent requirements on sample size (or shape) compared with other techniques such as optical absorption and reflection. (ii) The tunable radiation source provides a continuous photon energy range across the UV/VUV range that allows a more accurate and comprehensive survey of the band-edge features to be undertaken compared with conventional excitation methods. (iii) The radiation can be extended into the XUV energy range where the technique of x-ray absorption spectroscopy provides a probe of the local bonding environment (the K-edges of both B and N lie within the energy range 190–450 eV). This is particularly sensitive to sp^2 and sp^3 bonding in BN and the spectra can be recorded using bulk-sensitive luminescence yield [15, 16] as well as more conventional surface-sensitive electron yield methods. The advantage of using luminescence excitation, therefore, is that a self-consistent measurement method is available for determining *both* the sample's chemistry and structure *and* its band-gap energy. Furthermore, using the latest experimental advances, it is also now possible to image the luminescence emission and map the chemical state variation across the sample surface with sub-micron lateral resolution [17].

Luminescence excitation/emission spectroscopy has successfully been applied to a range of other wide-gap materials in order to probe electronic transitions close to the band-edge, such as aluminosilicates [18], CdS [19], InAlAs [20], EuSe [21] and SiO_2 [22]. The present work uses the methods developed in these previous studies to determine E_g for c-BN and h-BN.

2. Experimental details

The structural properties of the h-BN and c-BN used in this study were measured using standard XRD (Cu Kα, 1.542 Å: Bruker D8 Advance) and Raman spectroscopy (Jobin-Yvon LabRam, excitation wavelength, $\lambda = 632.8$ nm), and the uniformity and morphology of the c-BN microcrystals was confirmed using field-emission scanning electron microscopy. The stoichiometry was confirmed using x-ray photoelectron spectroscopy (Mg Kα, AEI-ES200) and the samples were found to have a very low level of surface C and O contamination.

Trans-band-gap excitation spectroscopy was carried out at 8 K in the energy range 4–20 eV on beamlines 3.2 and 3.1 at the UK synchrotron radiation source using a combination of two end-stations, MoLES [16] and CLASSIX1 [17]. The former provided high-resolution luminescence detection measurements on the volume-integrated emission, and the latter (a 2D imaging spectrometer system) was used to confirm the lateral uniformity of the luminescence excitation features. Optically detected x-ray absorption measurements were undertaken on beamline MPW6.1 at the same synchrotron radiation source, which covers both the B and N K-edges in the energy range 190–450 eV. High purity single-phase c-BN crystals (Element Six Ltd) were grown by high temperature, high pressure synthesis and consisted of uniform crystals of dimension $\sim$20 μm. The graphite-like h-BN samples consisted of commercially available high purity powder.

In all cases, materials were investigated without complex sample preparation; powders were attached to sample holders using conductive adhesive or hard-pressed into Al or Cu plates.

3. Results and discussion

3.1. Structural assessment via XRD and Raman spectroscopy

The x-ray diffraction spectra for BN samples are shown in figure 1(a) and are in good agreement with those published in the JCPDS data base for c-BN [23] and h-BN [24]. The full widths at half magnitude of most of the Bragg peaks of both samples are close to the instrumental resolution of 0.2°, indicating that there are no significant size-broadening effects present, although there is very slight unresolved broadening in some peaks such as the (002) and (111) in h-BN and c-BN respectively (h, k, l given as [23, 24]), as indicated by the insets to figure 1(a). This possibly suggests the presence of some micro-strain within the crystals. There is no evidence of contamination phases in either the c-BN or h-BN samples studied and, overall, the spectra verify the high quality of both samples.

The Raman spectra from BN are also well reported in the literature. Zinc-blende c-BN has one optical phonon at the centre of the Brillouin zone which is Raman active (Γ_{15}) and because of the ionic nature of the material, this splits into a TO and LO phonon. These Raman active phonons have been reported as having energies 1056 cm^{-1} (TO) and 1306 cm^{-1} (LO) [25, 26]. In the case of h-BN, there is a single first order Raman active mode of Γ_5 symmetry at an energy of 1364 cm^{-1} [27], and this is an excellent probe for the presence of hexagonal components in cubic material [28]. In our cubic samples, we have determined the positions of the Raman peaks as (1055 $\pm$ 7) cm^{-1} (TO) and (1305 $\pm$ 7) cm^{-1} (error bars correspond to FWHM). The line profiles can be fitted with a single Lorentzian curve and, under the highest sensitivity, there is no indication of a hexagonal component in the spectra. The linewidths and ratio of peak intensities are comparable with other data published on bulk high quality crystalline material. The spectra therefore confirm the crystalline nature of the materials and its phase purity. Unlike the case of c-BN, the Raman peak for the hexagonal phase shows a tail extending to low energies; this can be fitted to a pair of Lorentzian functions (peaking at 1363.5 and 1367.2 cm^{-1}), as seen in the inset of figure 1(b). The origin of such tails is uncertain, but they can be observed in other materials such as microporous silicon which contains a mixture of bulk and microcrystalline silicon [29].

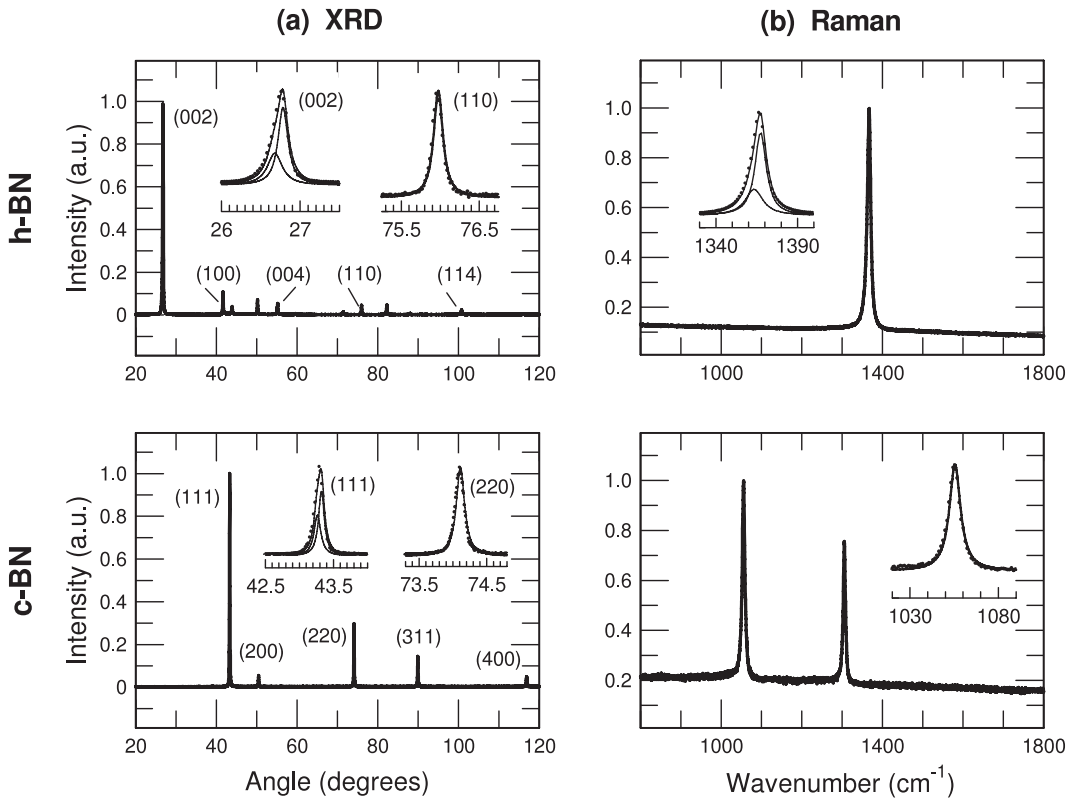

Figure 1. (a) X-ray diffraction patterns for the h-BN and c-BN samples used in the study. The insets show that the typical peaks in the spectra can be fitted to single Lorentzian line functions with a linewidth of 0.2°, close to the instrumental resolution limit, but the (002) and (111) peaks in h-BN and c-BN respectively are slightly broadened, with fitting possible to two unresolved Lorentzian functions. (h, k, l) diffraction peaks are labelled, following [23, 24]. (b) Raman spectra for the h-BN and c-BN samples. In the former, the peak can be fitted to two unresolved Lorentzians, and the latter to just a single Lorentzian peak.

3.2. X-ray excited luminescence emission and excitation (ODXAS)

In figure 2(a), the luminescence emission spectra are shown for both h-BN c-BN when excited at 190 eV. The spectra consist of a number of broad overlapping emission bands in the energy range 2–5 eV, and are typical for a range of materials studied in the course of the work (although the intensities of the various bands do change from between batches). For h-BN, the de-convoluted peaks occur at 3.07 and 3.82 eV (404 nm and 325 nm respectively) and in the c-BN, at 2.98, 3.28, 3.95 and 4.32 eV (416, 378, 314 and 287 nm respectively). The observation of much sharper, clearly defined, electron–phonon structure in the c-BN spectrum is further testament to its very high optical and structural quality. Such features are not generally observed in BN, but a good previous example where they are (using cathodoluminescence), is presented by Kanda *et al* [30]. In the present case, the highest energy c-BN emission displays partly-resolved phonon replicas with an average energy spacing of 0.152 eV: the zero-phonon energy line occurs at 4.93 eV (251 nm), but this is very weak; the replicas are more clearly defined, with the first phonon replica occurring at 4.794 eV. The phonon structure associated with the lower energy luminescence is better resolved, but the features are slightly obscured due to the overlap with the phonon replicas associated with the higher energy bands. They are more easily isolated in another c-BN sample in which this is the principal emission (the partial spectrum of which is shown also in figure 2(a)). In this case, the zero-phonon emission is definitively identified at 3.562 eV (348.1 nm), but there is clearly more than one phonon contribution to the replicas: the best defined has an energy of 0.155 eV, but there are other contributing phonons as low as 0.125 eV (hence the gradual spread in the replica structure on decreasing energy). In all cases, however, the phonon energies are similar to those of the LO lattice vibration energy as defined in the Raman experiments (1306 $\text{cm}^{-1} = 0.1619$ eV); the lower energy of the luminescence phonons is a reflection on the more localized defect vibrational states.

For the h-BN, an additional set of partly-resolved narrower emission peaks are observed in the energy range 5–5.8 eV, comprising of bands (FWHM 0.2 eV) at 5.32, 5.49 and 5.63 eV (233, 226, 220 nm). As the separation of these features is 0.15 eV, we assume that they are also LO phonon replicas of the zero-phonon emission at 5.63 eV. The actual nature of the defects contributing to these various emission processes is not the concern of the present work, but suffice it to say that they are similar to those previously reported using a variety of luminescence methods [30–34]. There appears to be no common agreement as to the actual assignation of specific defects with particular emission bands, although nitrogen vacancy-related centres are regarded as being prime candidates.

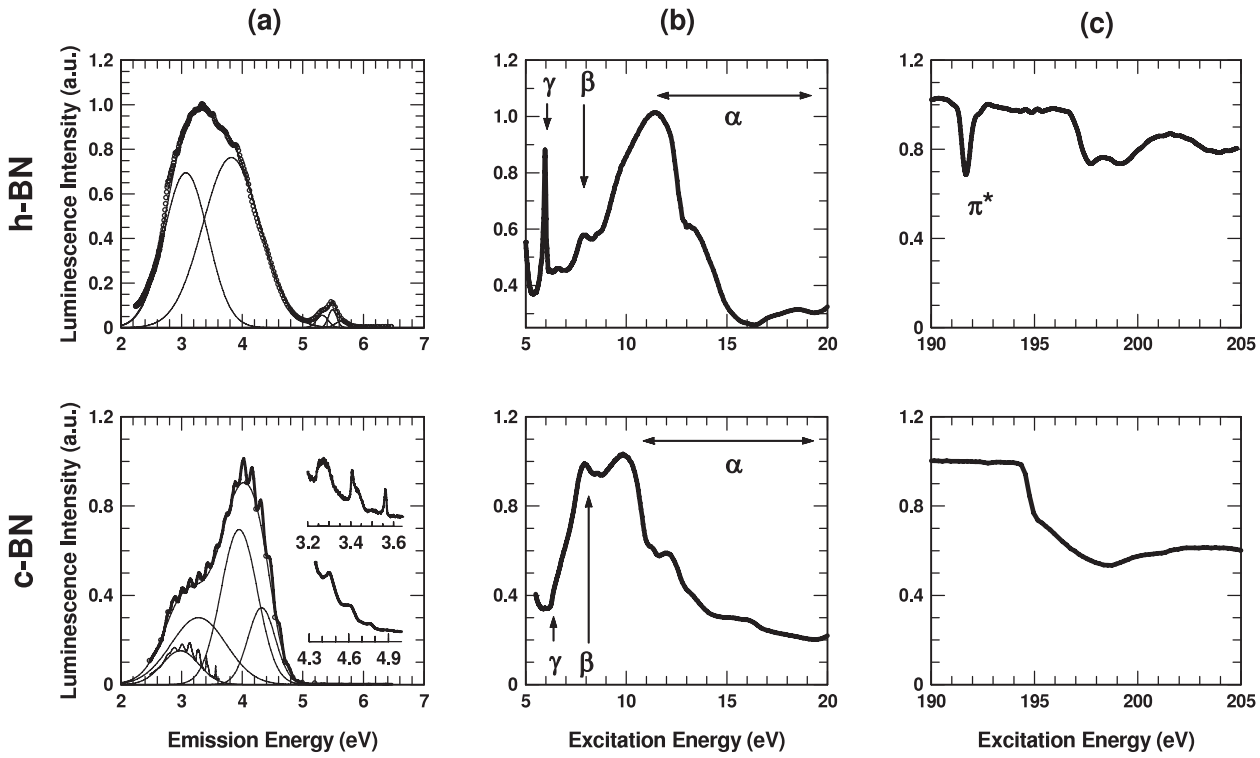

Figure 2. (a) Luminescence emission from the h-BN and c-BN samples, when excited using 190 eV XUV synchrotron light. The broad features are composed of a set of overlapping Gaussian bands. In c-BN, phonon structure is also observable, and the insets show details of these in higher resolution near the zero-phonon emission. The emission from a second c-BN sample, where only the 3 eV emission is observed, is used to highlight the phonon structure in the range 3.2–3.6 eV. (b) Luminescence excitation features of the h-BN and c-BN when exciting with synchrotron light in the range 5–20 eV, and detecting at 3.44 eV. The features α, β, γ are referred to in the text. (c) Luminescence excitation features of h-BN and c-BN when exciting with synchrotron light across the boron K-edge. The x-ray absorption spectra of the materials are carried by the luminescence, and can be used to verify the structural identity of the materials: the strong π^* resonance is only observed in sp^2-bonded h-BN.

Finally, the luminescence yield (detected in a broad band at 3.44 ± 0.38 eV; 360 nm, $\pm$40 nm) is considered as a function of the excitation energy when traversing the core-levels of the boron atoms (optically detected x-ray absorption spectroscopy, ODXAS). These are shown in figure 2(c) for both h-BN and c-BN. The h-BN is characterized by a prominent resonance at 192 eV, arising from excitation from the B 1s core level into unoccupied π^* states. This feature is entirely absent in pure σ-bonded c-BN, and confirms the structural integrity of each material in this study. (Its wider application to BN using wavelength-selectivity is described elsewhere [15].) The crucial point about the technique, however, is that the sample's structural identity is confirmed *via the same luminescence yield* in which the definitive band-gap measurements are to be extracted, as discussed in the following section.

3.3. Band-edge luminescence excitation spectroscopy

The broad features of the luminescence yield as a function of the incident synchrotron radiation from 5–20 eV are shown in figure 2(b) for both h-BN and c-BN whilst detecting emission at 3.44 ± 0.38 eV. These measurements reveal distinct features (labelled α, β, γ) associated with electronic processes that have not previously been accessible using luminescence excitation spectroscopy. However, strong anisotropy in the dielectric constant (and hence energy loss functions) for each material is known to occur in the energy range 8–20 eV [5, 35] with peaks especially apparent in the range 10–15 eV. These features correspond directly to the reduction in luminescence excitation efficiency observed here (marked 'α' in figure 2(b)) and they are also consistent with an increase in the absorption coefficient reported for c-BN [6].

The nature and magnitude of the optical band gaps is revealed by considering the emission and excitation data in the overlap region in more detail. In the range 5–7.5 eV the spectra for both materials display significant differences, as shown in figure 3(a). For h-BN, a prominent peak (γ of figure 2(b)) is observed at $\sim$6 eV (superimposed on a rising continuum), whereas for c-BN, a single step is observed at $\sim$6.3 eV, after which the excitation efficiency continues to rise up to 8 eV. These important features can be analysed more effectively following the removal of the continuum backgrounds, as shown in figure 3(b).

In contrast to standard optical absorption spectroscopy, the form of the luminescence yield as a function of excitation energy can be strongly dependent upon the emission band chosen for analysis, especially if there is competition for the available charge between different defects that may be present, and possible excitonic emission processes. In the case of

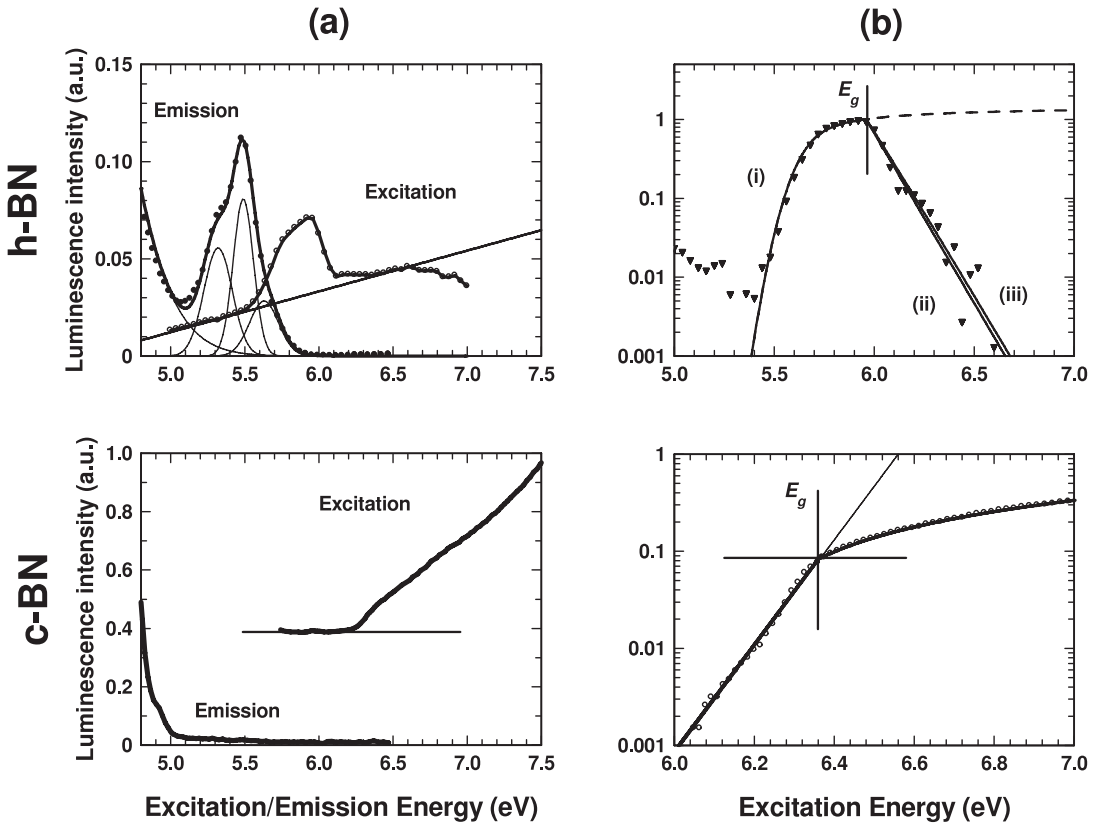

Figure 3. (a) Details of the high energy part of the emission, and low energy part of the excitation spectra in both h-BN and c-BN in the vicinity of the band-edge. (b) The band-edge luminescence excitation features of h-BN and c-BN, after the non-resonant backgrounds (shown by the lines in (a)) have been subtracted. In h-BN for excitation below the band-edge, the data (points) closely follow that expected from theory (solid curve, (i)), involving a direct band-gap material with both parabolic bands and shallow acceptors. Above E_g, the quantum yield reduces exponentially with excitation energy (curve (ii)) although this may be slightly modified if the contribution of defects is also considered (curve (iii)). For the c-BN, the results are typical of excitation from a material with no shallow defects; the band-edge is taken to be the intersect of the exponential sub-gap Urbach tail, and above-gap excitation (the solid curve fitted here to the data points as a linear dependence of the luminescence yield as a function of excitation energy).

SiO_2, for example, Itoh *et al* [22] showed that monitoring the defect and self-trapped exciton bands at 3 eV and 4 eV respectively, yielded almost diametrically opposed quantum yields, with the excitation spectrum of the excitonic emission essentially following the combined density of states of the conduction/valence bands, and the defect emission intensity falling rapidly for excitation energies greater than E_g. Similar effects have been demonstrated for the case of the various emission bands in $PbCl_2$ [36]. Nevertheless, the form of the sub band-gap excitation spectra are generally easier to define than for supra band-gap excitation, since the complexities of charge competition are reduced. In the following analyses, E_g is therefore taken to be the point at which the two excitation regimes meet; the complexities of the charge competition that yield variations in the supra-gap excitation profiles are not considered in the present work.

In the case of h-BN, the sub band-gap excitation profile can be accounted for by assuming the energy dependent absorption coefficient $\alpha(E)$ derives from excitation of charge from a relatively shallow acceptor centre, 5.62 eV below the conduction band minimum (with a Gaussian distribution of states, FWHM 0.20 eV) to a conduction band that is parabolic, i.e. the density of states varies as $(E - E_g)^{1/2}$. In this case, the luminescence intensity $L(E)$ varies as a function of the number of absorbed photons, i.e. $L(E) \propto (1 - \exp(-\alpha d))$, d being the sample thickness. This is plotted as curve (i) in figure 3(b), and well accounts for the experimental data in the energy range from 5.4 to 5.96 eV. Note that the parameters used for the acceptor centre used here, directly match the ground state of the defect giving rise to the near band-edge emission in the material, as shown in figure 3(a). Above 5.96 eV, the luminescence yield rapidly falls away and, as shown in the semi-log scale of figure 3(b), this is essentially exponential with energy (fitted as such to curve (ii)). Given the noise level on the data, it is not possible to ascertain whether this is exactly exponential in form, or whether there is a slight deviation if the additional contribution of the excitation of charge from the defects (dotted curve on figure 3(b)) is also taken into consideration (as given for curve (iii)). Nevertheless, in either case, the transition between sub- and supra-gap excitation is clear, and the value of the optical gap E_g for h-BN is determined to be 5.96 $\pm$ 0.04 eV. In respect of the wide range of values quoted in the literature from 4 to 6 eV [9], the closest this matches to any previous report is that of Watanabe *et al* [10] who determined a value of 5.97 eV at 8 K in purified h-BN material

capable of laser emission, using optical absorption over the range 5.6–6.0 eV.

Based on the luminescence emission spectra of figure 2(a), it is clear that there are a number of deep-lying defects in the material, and these will also contribute to the luminescence excitation profile, essentially by shifting curve (i) in figure 3(b) to lower energies. As such, in the excitation range close to the band-edge, the contribution of these defects is only weakly dependent on the excitation energy, and it is their presence that gives rise to the background excitation continuum apparent in figure 3(a).

In the case of c-BN, the absence of shallow defects provides a much cleaner trans-band-edge excitation profile, although the presence of deep-lying defects still yields a strong background continuum. As shown by the semi-log plot in figure 3(b), the luminescence yield increases exponentially in the range 6.0–6.3 eV, and this is typical of an Urbach tail deriving from transitions between band tail states below the fundamental absorption edge. Although the band edge is less distinct than in h-BN, as seen from figure 3(b), there is a clear deviation from the exponential rise in the luminescence yield at 6.36 ± 0.03 eV, above which (in the range 6.4–7 eV) it continues to rise as a linear function of excitation energy. We take the point of this deviation to represent the value E_g in the material.

The optical band-gap energies measured for c-BN and h-BN can briefly be considered in terms of their theoretical band-structures [1–5]. For h-BN, the strength and form of the resonances at 5.96 eV suggest a direct gap (or quasi-direct gap) transition, and this is most likely to be at H or K. It is not possible to resolve the smaller indirect H–M energy transition as this is likely to be considerably weaker. However, a second direct transition is predicted at Γ [5] with an energy of ∼8.9 eV and the weak feature at 7.9 eV (marked β in figure 2(b)) could relate to this transition. For c-BN, the value of 6.36 eV corresponds to the smallest indirect Γ–X energy transition, but a direct transition at Γ is also predicted to occur at ∼8.7 eV. In figure 2(b), the luminescence yield increases steadily from 6.36 eV to a maximum at 7.9 eV (marked γ and β) and so β may represent the direct gap Γ absorption edge in c-BN. Finally, it is relevant to note that, if 6.36 eV does represent an *indirect* transition, there is no evidence from the data for the ± phonon contributions to the transition, and this is true also for the experimental data taken at higher temperatures.

4. Conclusion

The deployment of synchrotron radiation has been shown to be highly effective in probing the near band-edge structure of boron nitride, using luminescence excitation spectroscopy methods. Using a combined luminescence emission/absorption approach, it has been possible to accurately determine the band-gap energies, E_g, for both hexagonal and cubic varieties of the material. The indirect Γ–X optical band-gap transition in cubic boron nitride is determined to be (6.36 ± 0.03) eV, and the quasi-direct band-gap energy in hexagonal boron nitride is determined to be (5.96 ± 0.04) eV. The quality of the materials studied, in terms of both purity and structure, has been verified by a number of different techniques, and the values of E_g obtained are therefore considered to be definitive. The quality assurance methods include both Raman scattering and x-ray diffraction, but the chemistry and structure is also confirmed self-consistently via luminescence excitation spectroscopy across the core-level energies of boron (optical detection of x-ray absorption). These measurements confirm that the luminescence (from which the band-gap energies are derived) originate exclusively from pure h-BN and c-BN phases in the two sample types respectively.

Acknowledgments

This work was carried out within the Centre for Advanced Functional Materials and Devices (CAFMaD) and has been supported by the UK research councils EPSRC (grant EP/C511212/1) and CCLRC (beamtime awards 42015 and 45090). Element Six Ltd are thanked for the provision of high quality BN material. We are also grateful for the comments on the script by an anonymous referee, resulting in an improved interpretation of the results.

References

[1] Dovesi R, Pisani C, Roetti C and Dellarole P 1981 *Phys. Rev.* B **24** 4170
[2] Furthmuller J, Hafner J and Kresse G 1994 *Phys. Rev.* B **50** 15606
[3] Liu L, Feng Y P and Shen Z X 2003 *Phys. Rev.* B **68** 104102
[4] Robertson J 1984 *Phys. Rev.* B **29** 2131
[5] Xu Y N and Ching W Y 1991 *Phys. Rev.* B **44** 7787
[6] Miyata N, Moriki K, Mishima O, Fujisawa M and Hattori T 1989 *Phys. Rev.* B **40** 12028
[7] Chrenko R M 1974 *Solid State Commun.* **14** 511
[8] Solozhenko V L, Lazarenko A G, Petitet J P and Kanaev A V 2001 *J. Phys. Chem. Solids* **62** 1331
[9] Akamaru F, Onodera A, Endo T and Mishima O 2002 *J. Phys. Chem. Solids* **63** 887
[10] Watanabe K, Taniguchi T and Kanda H 2004 *Nat. Mater.* **3** 404
[11] Agui A, Shin S, Fujisawa M, Tezuka Y, Ishii T, Muramatsu Y, Mishima O and Era K 1997 *Phys. Rev.* B **55** 2073
[12] Tarrio C and Schnatterly S E 1989 *Phys. Rev.* B **40** 7852
[13] Zhang W J and Matsumoto S 2001 *J. Mater. Res.* **16** 3430
[14] Zhou X T, Sham T K, Chan C Y, Zhang W J, Bello I, Lee S T and Hofsass H 2006 *J. Appl. Phys.* **100** 014909
[15] Evans D A, Vearey-Roberts A R and Poolton N R J 2006 *Appl. Phys. Lett.* **89** 161107
[16] Quinn F, Poolton N, Malins A, Pantos E, Andersen C, Denby P, Dhanak V and Miller G 2003 *J. Synchrotron Radiat.* **10** 461
[17] Poolton N R J, Towlson B M, Hamilton B and Evans D A 2006 *Nucl. Instrum. Methods* B **246** 445
[18] Malins A E R, Poolton N R J, Quinn F M, Johnsen O and Denby P M 2004 *J. Phys. D: Appl. Phys.* **37** 1439
[19] Ullrich B, Bagnall D M, Sakai H and Segawa Y 1999 *Solid State Commun.* **109** 757
[20] Roura P, Lopez de Miguel M, Cornet A and Morante J R 1997 *J. Appl. Phys.* **81** 6916
[21] Akimoto R, Kobayashi M and Suzuki T 1996 *J. Phys.: Condens. Matter* **8** 105
[22] Itoh C, Tanimura K, Itoh N and Itoh M 1989 *Phys. Rev.* B **39** 11183
[23] Bundy F P and Wentorf R H 1963 *J. Chem. Phys.* **38** 1144
[24] Pease R S 1952 *Acta Crystallogr.* **5** 356

[25] Alvarenga A D, Grimsditch M and Polian A 1992 *J. Appl. Phys.* **72** 1955
[26] Eremets M I, Gauthier M, Polian A, Chervin J C, Besson J M, Dubitskii G A and Semenova Y Y 1995 *Phys. Rev.* B **52** 8854
[27] Geick R, Perry C H and Rupprecht G 1966 *Phys. Rev.* **146** 543
[28] Reich S, Ferrari A C, Arenal R, Loiseau A, Bello I and Robertson J 2005 *Phys. Rev.* B **71** 205201
[29] Goodes S R and Jenkins T E 1988 *J. Microcomput. Appl.* **11** 57
[30] Kanda H, Ono A, Suda Y and Era K 1997 *Mater. Sci. Forum* **258–263** 1265
[31] Kawaguchi M, Nozaki K, Kita Y and Doi M 1991 *J. Mater. Sci.* **26** 3926
[32] Manfredotti C, Vittone E, Lo Giudice A, Paolini C, Fizzotti F, Dinca G, Ralchenko V and Nistor S V 2001 *Diamond Relat. Mater.* **10** 568
[33] Taylor C A, Brown S W, Subramaniam V, Kidner S, Rand S C and Clarke R 1994 *Appl. Phys. Lett.* **65** 1251
[34] Zhang W J, Kanda H and Matsumoto S 2002 *Appl. Phys. Lett.* **81** 3356
[35] Cappellini G, Satta G, Palummo M and Onida G 2001 *Phys. Rev.* B **64** 035104
[36] Kink R, Avarmaa T, Kisand V, Lõhmus A, Kink I and Martinson I 1998 *J. Phys.: Condens. Matter* **10** 693